An Adaptive Slicing Algorithm for Profiled Edge Laminae Tooling

Seungryeol Yoo[1,#] and Daniel Walczyk[2]

1 School of Mechanical Engineering, Korea Univ. of Technology and Education, Byeongcheon-myeon, Chungcheongnam-do, Chenoan, South Korea, 330-708
2 Department of Mechanical, Aerospace and Nuclear Engineering , Rensselaer Polytechnic Institute , 110 8TH ST, Troy NY, USA, 12180-3590
Corresponding Author / E-mail: yoos@kut.ac.kr, TEL: +82-41-560-1168, FAX: +82-41-560-1253

KEYWORDS: Rapid Tooling, Profiled Edge Laminae Tooling, Layer-Slicing Algorithm, Shape Error Measurement

Of all the rapid tooling (RT) methods currently available, thick-layer laminated tooling is the most suitable for large-scale, low-cost dies and molds. Currently, the determination of a lamina's contour or profile and the associated slicing algorithms are based on existing rapid prototyping (RP) data manipulation technology. This paper presents a new adaptive slicing algorithm developed exclusively for profiled edge laminae (PEL) tooling. PEL tooling is a thick-layer RT technique that involves the assembly of an array of laminae, whose top edges are simultaneously profiled and beveled using a line-of-sight cutting method based on a CAD model of the intended tool surface. The cutting profiles are based on the intersection curve obtained directly from the CAD model to ensure geometrical accuracy. The slicing algorithm determines the lamina thicknesses that minimize the dimensional error using a new tool shape error index. At the same time, the algorithm considers the available lamination thicknesses and desired lamina interface locations. We demonstrate the new slicing algorithm by developing a simple industrial PEL tool based on a CAD part shape.

Manuscript received: October 30, 2006 / Accepted: April 30, 2007

1. Introduction

Since the development of stereolithography in 1986[1], the layer-by-layer build technique used in rapid prototyping (RP) has also proven to be useful for rapid tooling (RT). RT evolved from the application of RP technology, and is essentially RP-driven tooling. Although many different RT methods have been developed and commercialized in the last decade, most applications have focused on relatively small-scale tooling in which 'conventional' high-speed CNC machining of a solid billet of material is still well suited.[2] We believe that this situation, among other factors, has hindered widespread industrial acceptance of RT. Very few layer-based RT methods have proven to be suitable for large-scale tooling applications. This is an unfortunate situation since most conventional tooling fabrication methods at this scale, such as CNC machining or casting, involve long lead-times and cost. One notable exception is thick-layer laminated tooling, which uses layers thicker than 1.0 mm, primarily because of the commercial availability of multiaxial CNC cutters (*e.g.*, lasers or abrasive waterjets) with workbeds that are large enough to cut individual laminae out of a variety of sheet materials.

Profiled edge laminae (PEL) tooling is a thick-layer laminated tooling method that was developed by Walczyk and Hardt[3,4] primarily for large tooling applications. As illustrated in Fig. 1(a), this RT method involves assembling an array of laminae—each one with a uniquely profiled and beveled top edge—together in a precise and repeatable manner by registering each lamina's bottom edge and an adjacent side edge to a fixture with two precisely machined reference planes oriented 90° apart (see Fig. 1(b)). The profiling and beveling of each lamina's top edge is accomplished simultaneously using a 'line-of-sight' cutting process (*e.g.*, abrasive waterjet machining, cutting with a Nd:YAG pulsed laser, plasma cutting, or wire EDM) capable of oblique cutting, which leaves a piecewise continuous tool surface perpendicular to the laminae interfaces (see Fig. 1(c)). Although other cutting methods, such as laser cutting, have been investigated for oblique cutting[5], abrasive waterjet (AWJ) cutting is preferred over other cutting processes since the bevel geometry and surface finish are more consistent and fewer restrictions exist on what tool materials can be cut.[4,6] Once they are cut, the array of PELs is then clamped, as shown in Fig. 1(d), and/or bonded (*e.g.*, by brazing) into a rigid laminated tool.

PEL tooling offers advantages over CNC machining of a solid billet of material, including easy reconfigurability and the ability to route conformal heating/cooling channels and process sensors (*e.g.*, temperature) or incorporate special features such as vacuum lines. Many of these tooling features are illustrated in Fig. 1(b). PEL tooling also allows for variable lamina thicknesses to be used throughout the tool. As shown in Fig. 2, a tooling designer may wish to vary the lamina thickness in a laminated tool in the following situations:

- to specifically locate lamina interfaces at which a vertical wall, sharp geometrical change, process sensor (*e.g.*, temperature, pressure), and/or other specialized geometrical features are required;
- to use thinner laminae in tool surface regions with high slope angles or dramatically changing geometrical features, thereby reducing the dimensional shape error due to straight beveling; and
- to use thicker laminae in tool surface regions with low slope angles and very gentle curvatures, thereby reducing the number of laminae that must be handled and, in many cases, the cutting time

required.

Situation #1 typically requires specific inputs from the tooling designer. Situations #2 and #3 require some effective means of estimating the localized dimensional shape error of a PEL tool as a function of the lamina thickness.

The development of a PEL tool for use in large-scale part manufacturing (*e.g.*, a thermoforming mold for interior aircraft panels) involves detailed designs produced using CAD software followed by computer-controlled fabrication (*e.g.*, individually machining lamina from aluminum sheet stock using a five-axis CNC AWJ cutting machine). The maximum allowable shape tolerances (*e.g.*, ±0.01 mm) are established during the tooling design phase. Conformance of the fabricated PEL tool shape to the specified tolerance is based on the original CAD model. If the tool shape is simple (*e.g.*, a half-cylinder), the dimensional shape error depends mainly on the accuracy of the fabrication machine. Conformance to a specified tolerance is simply a matter of choosing an appropriately accurate machine. However, if the tool shape is a complex 3-D surface, as is usually the case, the dimensional shape error depends not only on the machine accuracy, but also on the cutting trajectory algorithm (*i.e.*, the method used to develop suitable cutting trajectories for CNC AWJ machining of the profiled and beveled top edge of each lamina) and the layer slicing algorithm used.

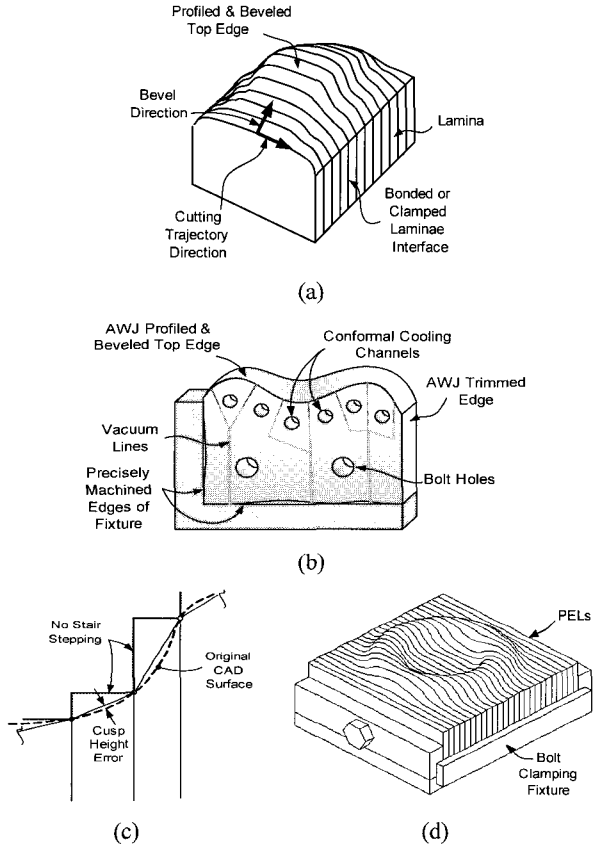

Fig. 1 Schematic diagrams of (a) an unclamped PEL tool, (b) fixturing (*e.g.*, for cutting) and a registration scheme for individual lamina, (c) a section view showing the piecewise continuous nature of a PEL tool with resulting cusp-height error, and (d) the clamping of a laminae array into a rigid tool

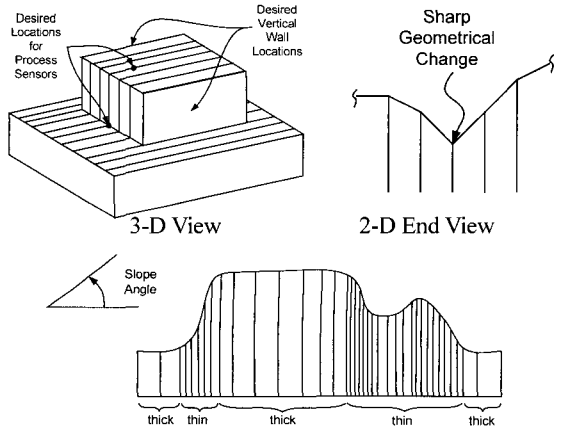

Fig. 2 Reasons for varying the lamina thickness in a PEL tool

While the machine accuracy and cutting trajectory generation are important to PEL tooling development, this paper focuses on the issue of layer slicing and how it impacts both the tool design and accuracy. Specifically, a new adaptive slicing algorithm for PEL tooling is presented with particular emphasis on the dimensional shape error estimation and other practical design considerations. This new algorithm was developed because existing algorithms available in the literature are unsuitable for PEL tooling.

2. Background on Layer Slicing and Error Estimation

Since the focus of this paper is on layer slicing for PEL tooling, it is useful to review the state of the art related to layer slicing algorithms for RP technologies. Slicing algorithms developed for RP have focused primarily on reducing the cusp-height error associated with RP's inherent layer-to-layer stair-stepping effect by optimizing the slicing thickness. Suh and Wozny[7] introduced an adaptive slicing algorithm to reduce 3-D aliasing or stair-stepping by determining layer heights based on the cusp-height error between each layer contour and the exact CAD geometry. Kulkarni and Dutta[8] developed a procedure for adaptively slicing parameterizable algebraic surfaces and applied it to layered manufacturing processes. The main parameter used to determine the variable layer slice thickness was the normal curvature in the vertical direction. Zhao and Laperriere[9] developed an adaptive direct slicing method that enabled model part fabrication with high accuracy and production efficiency. The method generated precise contours for each layer from the solid model while modifying the layer thickness to consider the curvature of the surface of the solid model in the vertical direction. This reduced the stair-stepping effect and decreased the number of layers.

Almost all of the prior work dealing with adaptive layer slicing has been for layers characterized by 2-D continuous contours with perpendicular (*i.e.*, non-beveled) edges. Consequently, the layer slicing algorithms have focused on reducing the chordal deviation inherent to the stair-stepping effect. This includes other layer-based RP and RT methods, such as laminated object manufacturing. Unfortunately, these algorithms are of little use to PEL tooling due to its inherent edge beveling.

With PEL tooling, each layer or lamina is characterized by a noncontinuous profile of the top edge and beveling between adjacent lamina profiles, which eliminates most of the error associated with the stair-stepping effect, as shown in Fig. 1(c). To reduce the remaining error associated with thick beveled-edge layers, an effective method to evaluate the dimensional shape error between the original tool CAD model and the intended PEL tool surface is required. Several inspection methods have been developed to evaluate shape errors between a 3-D CAD surface model and the resulting machined surface. A method proposed by Huang *et al.*[10] to compare measured and referenced surfaces consisted of two iterative operations: constructing a pseudo transformation matrix from measurement data and reference points, and obtaining reference points from the transformation matrix. This iterative method required significant computational time. Kase *et al.*[11] developed local and global evaluation methods for free-form surfaces. The local evaluation method used the change in the principal curvatures between the original CAD data and the actual surfaces, such as the results of numerical simulations or measured data of actual formed samples. The global evaluation method used aggregate normal vectors to characterize a portion of the surfaces. This method, based

on the change of the curvature and normal vectors, does not provide a good comparison for the differential distances between a CAD surface and the profiled and beveled top edge of a PEL tool. Hur and Lee[12] developed a skull RP model using a laser scanner. They reconstructed a 3-D CAD model with an STL file format from measurement data. Since the true volumetric error was the deviation between the CAD model and the actual surface, if the reconstructed CAD model provided good accuracy, it could be used to evaluate the actual surface.

3. Adaptive Slicing Algorithm

The adaptive slicing algorithm is part of a comprehensive CAD-based PEL tooling development process developed by Yoo[13] as an improvement to the work of Im and Walczyk.[14] A flowchart of the complete tooling development process and slicing algorithm is shown in Fig. 3. The entire process begins by creating a CAD model of an initial tool surface based on the part shape and manufacturing process(es) used to fabricate the part. In general, the adaptive slicing algorithm is used to choose an initial slicing reference plane, manage lamination stock sizes, slice the CAD surface model, compute the dimensional errors, and adjust the lamina thickness so as not to exceed a chosen dimensional error limit. The slicing reference plane is first selected based on the tooling designer's intuition and experience; this will be discussed in more detail in Section 3.1. The available lamina thickness stock sizes and their inherent thickness tolerances must also be considered. Based on this information, the adaptive slicing algorithm selects the optimal lamination thickness that minimizes the dimensional error. This feature will be discussed in more detail in Section 3.2.

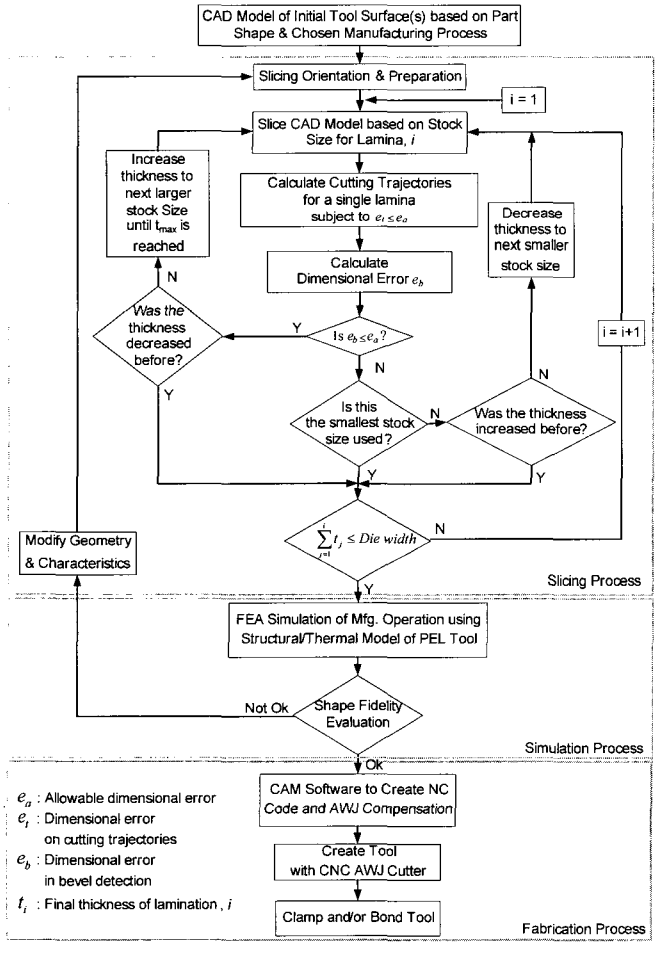

Fig. 3 Flowchart of the PEL tool development process and adaptive slicing algorithm

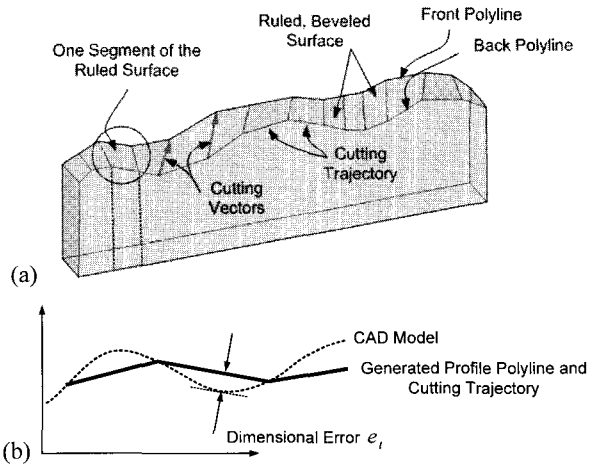

Fig. 4 (a) Lamina geometry (*i.e.*, front and back profile polylines connected with a ruled and beveled surface) used by the adaptive slicing algorithm and (b) dimensional error measured along the cutting trajectory

Each PEL tool lamina has a ruled and beveled top edge defined by a pair of polyline profiles, as shown in Fig. 4(a). Polylines, whose nodes (*i.e.*, segment endpoints) are extracted directly from the CAD model of the tool surface, are used to define the profile edges for the cutting trajectory generation algorithm.[13] Since each cutting trajectory consists of tool vectors and a tool profile, it can be used to create compensated AWJ cutting trajectories and the corresponding NC code directly. A user-defined error value (e_a) limits the allowable chordal deviation (e_t) of the profile polylines from the original CAD model (*i.e.*, reference shape), as shown in Fig. 4(b), along the cutting trajectory direction (defined in Fig. 1(a)).

Although the adaptive slicing algorithm is shown schematically in the *Slicing Process* block of Fig. 3, a more detailed description is provided in Table 1. Before the lamina slicing process begins, the allowable dimensional error (e_a), allowable stock lamina thicknesses, default lamina thickness, and slicing reference plane must be chosen. For design convenience, the allowable error (e_a) is also used to limit the bevel direction error (e_b), although separate error limits can be used for e_t and e_b if required. Both shape errors are measured using the original CAD model and a virtual representation of the PEL tool surface. In general, the error limit e_a (0.01 mm is a typical value) is based on the manufacturing process to be used, tolerance specifications for the manufactured component, and overall size of the PEL tool. After the slicing orientation and all necessary parameters have been chosen, the slicing procedure begins with a starting lamina thickness. If the available stock sizes are simply increased by a standard size (discussed in the next paragraph), then all possible profile polylines can be generated beforehand and this information will be stored in the computer memory at the very start of the slicing process (*i.e.*, Step 2 in Table 1). If the stock sizes are not based on a standard increment, then Steps 3 and 4 for generating profile polylines must be repeated for each iteration of the algorithm, which is less efficient from a computational viewpoint.

An important consideration in slicing a PEL tool is the choice of the lamina thickness. Although sheet or plate material can be machined or ground to obtain any specific lamina thickness, this is both an expensive and unnecessary procedure. A more practical approach is to use commercially available stock thicknesses instead. One of the easiest ways to slice a tool is to use stock thicknesses based on a standard size increment that are readily available from a commercial vendor. For example, a standard size increment of 5 mm suggests stock laminae thicknesses of 5, 10, 15, and 20 mm, *etc.* A standard stock size increment is also very useful in developing a practical slicing algorithm for PEL tooling. Since the advanced slicing algorithm searches for an optimal lamina thickness, generating all possible laminae profiles (and their corresponding midplane

Table 1 PEL lamina slicing algorithm as depicted in the *Slicing Process* block of Fig. 3

Step	Procedure
1	Specify the allowable dimensional error e_a, allowable stock lamina thicknesses, default lamina thickness, and slicing reference plane. Let $i = 1$ for the first lamina of the PEL tool as shown in Fig. 3. Also, choose a starting lamina thickness, which is usually one of the middle stock thicknesses (*e.g.*, 3 mm for stock thicknesses of 1, 2, 3, 4, and 5 mm).
2	Slice the entire CAD model of the tool surface perpendicular to the slicing reference plane by spacing all other slicing planes using the standard size increment. The nodes of each polyline profile are stored sequentially in the computer memory.
3	Extract the slice information for lamina i based on the previous lamina thickness. See Ref. (13) for specific details.
4	Calculate the cutting trajectories for lamina i subject to the $e_t \leq e_a$ rule. See Ref. (13) for specific details.
5	Calculate the dimensional error e_b as discussed in Section 3.2.
6	Determine the actual slice thickness. Except for $i = 1$, the assumed thickness for lamina i to start the iteration process is that of the previous one, $(i - 1)$. As shown in Fig. 2, if $e_b < e_a$, the lamina can be made thicker up to the maximum allowable stock thickness t_{max}. If $e_b > e_a$, the lamina can be made thinner down to the minimum allowable stock thickness t_{min}. The condition loops "Was thickness previously increased?" and "Was thickness previously decreased?" are added to avoid endless looping once the algorithm has converged to an optimal lamina thickness t_i.
7	Check if the entire PEL tool has been sliced. After finding each optimal thickness t_i, compare the width (*i.e.*, the z-direction dimension in Figs. 10 and 11) of the tool's CAD model (designated as *DieWidth*) with the current total sliced lamina thickness, *i.e.*, $\sum_{j=1}^{i} t_j$. If $\sum_{j=1}^{i} t_j < DieWidth$, then repeat Steps 3–6 and increment lamina number by 1 (i.e. $i = i + 1$). Otherwise, the slicing is finished.

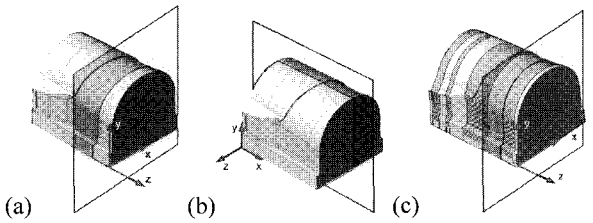

Fig. 5 Two possible slicing orientations considered for a composite lay-up mold: (a) Case I and (b) Case II. (c) Final orientation and resulting slice thicknesses from Ref. 15

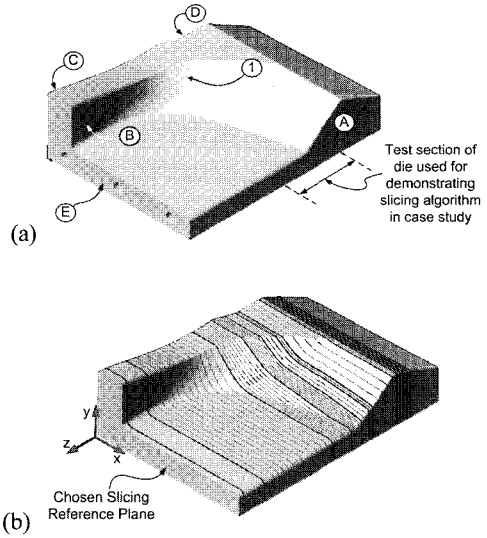

Fig. 6 (a) Slicing reference plane choices for a hydroforming die and (b) the resulting PEL slicing

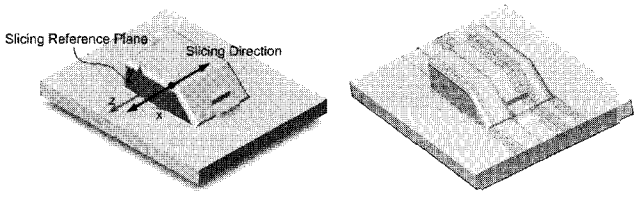

Fig. 7 (a) Thermoforming mold with an inner vertical wall used as the slicing reference plane and (b) the resulting sliced tool

profiles) based on a standard stock size increment before starting the actual slicing algorithm actually reduces the computational time.

3.1 Slicing Orientation and Preparation

Laminae interfaces are affected by the choice of the slicing orientation and the slicing reference plane. The slicing orientation also affects the stiffness of the PEL tool, accuracy of the machining, and complexity of the cutting trajectories.

Slicing Orientation. When deciding on a slicing orientation, existing vertical walls in the CAD model of the PEL tool surface can serve as slicing reference planes. This principle was applied for a composite lay-up and curing mold for graphite/epoxy knee brace components. Brown[15] considered two possible slicing orientations, as shown in Fig. 5. Case I (Fig. 5(a)) gave more desirable laminae geometries than Case II (Fig. 5(b)) from an AWJ-cutting perspective. Brown eventually selected the Case I orientation, as shown in Fig. 5(c) to fabricate this PEL mold.

Slicing Reference Plane. The following example demonstrates how a slicing reference plane is chosen. An aluminum die used to hydroform sheet metal parts for the aircraft industry is shown in Fig. 6(a). It has five vertical surfaces (denoted as A, B, C, D, and E) that can be considered for the slicing reference plane. Surface E is the best choice in this example since choosing surfaces A, B, C, or D results in a slicing orientation that makes it difficult to match adjacent bevels in the area of the tool surface denoted by "1" in Fig. 6(a). The resulting sliced PEL die is shown in Fig. 6(b). Brown[15] fabricated an actual PEL tool and used it to hydroform aluminum parts. These were compared with parts hydroformed using a CNC-machined tool.

Often, the slicing reference plane is an outer vertical wall of a tool, as was the case in the preceding example. However, situations occur when an inner vertical wall should be considered. Figure 7(a) shows a CAD model of a mold used to thermoform a plastic housing used in a commercial photograph scanning/enlarging/printing machine. The mold has two distinct inner vertical walls. When one of these walls was chosen as the slicing reference plane, slicing occurred on both sides of the normal direction to this plane, *i.e.*, in the $\pm z$-direction. The resulting sliced PEL mold is shown in Fig. 7(b).

3.2 Overall Dimensional Error of a Lamina in the Bevel Direction

Each PEL tool lamina has a ruled and beveled top surface that is defined by a front and a back polyline profile, as shown in Fig. 4(a). The shape fidelity of the beveled top surface cannot be effectively compared to the original CAD surface using the dimensional error e_t because it only quantifies the chordal deviation along the cutting

trajectory. Therefore, another shape error tolerance index e_b is used to measure the volumetric deviation between the CAD surfaces model and the beveled PEL tool surface.

To evaluate e_b between the PEL and CAD surfaces, let us focus on one segment of the ruled PEL surface, *e.g.*, the beveled edge segment circled in Fig. 4(a). As shown in Fig. 8, the actual volumetric deviation for this segment is defined as the volume created between the CAD tool surface and PEL ruled surface, which are bounded by four vertical planes (*i.e.*, two edges of the ruled surface segment and both lamina interfaces). Although it is possible to calculate the volumetric deviation for each segment, it is not practical due to the computational complexity involved. A simpler method that still effectively estimates the volumetric deviation is to measure the linear deviation between the two surfaces along vertical rays at predefined positions. These reference positions are uniformly spaced on a grid in the x–y plane by a length δ based on the dimensional characteristics of the lamina, thereby forming a uniform matrix of measurement points. A ray is essentially a vertical line through reference positions $R_{i,j}$ predefined on the bottom x–z plane of the PEL model. It intersects both the beveled top surface of the PEL and the original CAD surface. The local surface dimensional error $(e_b)_{i,j}$ is defined as the distance along the ray between the two surface intersections according to the relation

$$(e_b)_{i,j} = \left|(H_{PEL})_{i,j} - (H_{CAD})_{i,j}\right| \tag{1}$$

where $(H_{PEL})_{i,j}$ is the vertical (*i.e.*, y-direction) height of the intersection between the ray and the PEL ruled surface, and $(H_{CAD})_{i,j}$ is the vertical height of the intersection between the ray and the CAD tool surface.

The overall dimensional error e_b for a particular bevel segment or an entire lamina is defined as the root mean square (RMS) value of all local surface dimensional errors according to the relation

$$e_b = \sqrt{\frac{\sum_{j=1}^{m}\sum_{i=1}^{n}\left[(e_b)_{i,j}\right]^2}{nm-1}} \tag{2}$$

where n and m are the number of rays in the matrix in the x- and z-directions, respectively. Since e_b, as defined by Eq. (2), is an overall measure of the surface deviation for a set of equally spaced grid positions, we hypothesize that it will give more evenly distributed errors over the tool surfaces than other methods. For example, if the dimensional error is measured along the bevel directions (*i.e.*, along the cutting vectors), the dimensional error will be too heavily weighted in areas of the tool surface that have many cutting vectors due to dramatic changes in the surface curvature.

3.2.1 Measuring Surfaces of the CAD Model

To measure the top surface of CAD models, reference positions are selected from the model x–z plane. As shown in Fig. 9, the position $(H_{CAD})_{i,j}$ in the y-direction is defined by the intersection of the CAD surface with a vertical ray located at matrix position (i,j). For example, suppose that a section with depth = 76 mm (3"), width = 191 mm (7.5"), and height = 61 mm (2.4") of the sheet metal forming die shown in Fig. 6 is to be measured. The die section is shown in Fig. 10(a). The intersections are measured for a SolidWorks CAD model using the API function *ModelDoc2.RayIntersections*. For each ray, the *base points*, *vector*, *offset*, and *object* must be defined. In this case, the *base points* are the reference positions of the point matrix on the x–z plane with a spacing of δ = 6.4 mm (0.25"), the directional vector is $[x\ y\ z]$ = [0 1 0], and the *object* is the CAD model. The measured $(H_{CAD})_{ij}$ positions of the CAD model are shown as the upper cloud of points in Fig. 10(b).

3.2.2 Measuring Surfaces of the Virtual PEL Tool

The top surface of each lamina is a segmented surface defined by a pair of cutting trajectories and a series of cutting vectors, as shown in Fig. 11. "Line-of-sight" cutting (*e.g.*, AWJ cutting) will follow

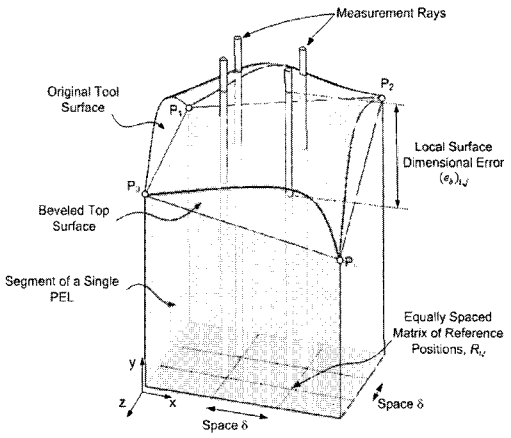

Fig. 8 Definition of the vertical linear deviation $(e_b)_{i,j}$ between a segment of the PEL's ruled surface geometry and the original tool surface geometry

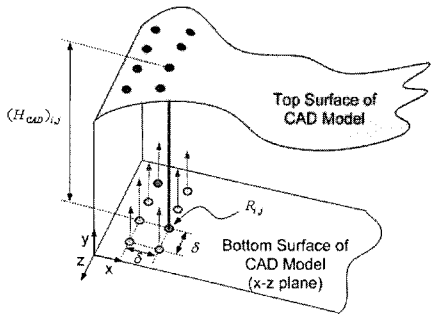

Fig. 9 Matrix of reference positions for measuring rays

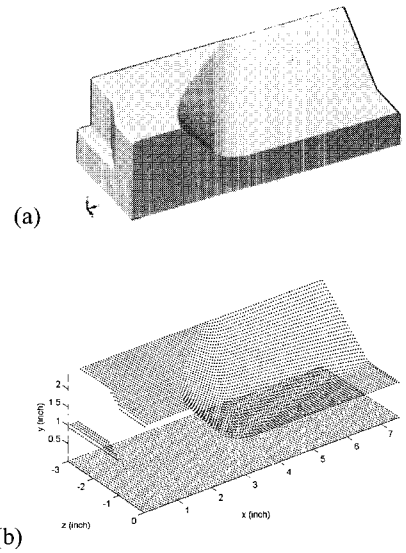

Fig. 10 Example of measuring the top surface of a CAD model: (a) actual model of the tool section and (b) the $(H_{CAD})_{ij}$ points of the tool forming surface measured on a x–z grid with a spacing of δ = 1.91 mm (0.075")

either the front or back cutting trajectory as determined during the CAM development stage with a nozzle orientation based on the cutting vectors. The cutting orientation is typically interpolated between the cutting vectors in a linear fashion by the CNC machine controllers. A ray at reference position $R_{i,j}$ intersecting a segment of a lamina's top beveled edge was considered to determine how to measure $(H_{PEL})_{i,j}$, as shown in Fig. 12.

Two cutting trajectory segments, P_1P_2 and P_3P_4, and two cutting vectors, P_1P_3 and P_2P_4, define each segment of the ruled beveled top edge, as shown in Fig. 12. Several ray reference positions are also

contained within each segment. Since these vectors and trajectories are known, the four points and their coordinates on the k^{th} beveled surface (*i.e.*, P_1, P_2, P_3, and P_4 with coordinate origin for the lamina as shown) are also known. The point of intersection $(H_{PEL})_{i,j}$ can be determined from the ray reference position $R_{i,j}$ on the x–z plane and the k^{th} beveled surface. When the k^{th} segment is projected onto the x–z plane yielding points Q_1, Q_2, Q_3, and Q_4, we can determine (u, w, v) that satisfy

$$R_{i,j} = (1-w)\{(1-u)Q_1 + uQ_2\} + w\{(1-v)Q_3 + vQ_4\}, \quad (3)$$

where $0 \le u \le 1$, $0 \le v \le 1$, and $0 \le w \le 1$. Since Q_1Q_2 and Q_3Q_4 are parallel, the query points Q_1, Q_2, Q_3, and Q_4 on the k^{th} projected plane have the following constraints:

$$\begin{aligned} Q_{1y} &= Q_{2y}, \\ Q_{3y} &= Q_{4y}, \\ \text{and } ((1-u)Q_1 + uQ_2)_x &= ((1-v)Q_3 + vQ_4)_x. \end{aligned} \quad (4)$$

With $(u, v$ and $w)$, the project image of $R_{i,j}$ can be obtained as

$$(H_{PEL})_{i,j} = (1-w)\{(1-u)P_1 + uP_2\} + w\{(1-v)P_3 + vP_4\} \quad (5)$$

4. Case Study

The adaptive slicing algorithm developed in Section 3 was applied to the development of the industrial production tool shown in Fig. 6. This tool is a used as a die for hydroforming aluminum aircraft parts. All programming was performed using Matlab by MathWorks and SolidWorks API functions. The preferred PEL slicing orientation for this die is along the z-direction, as shown in Fig. 6(b). Except for the *Test Section* identified in Fig. 6(a) and shown by itself in Fig. 10(a), all sections of this hydroforming die require relatively simple cutting trajectories to make the corresponding laminae. The *Test Section* is definitely the most challenging section of the die, and hence, it is the focus of this production tool case study.

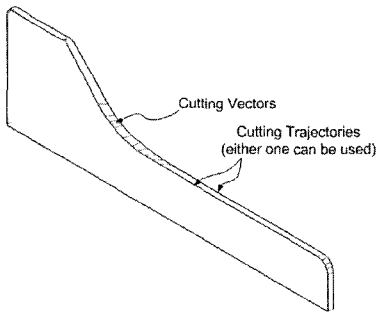

Fig. 11 Example of a lamina defined by cutting trajectories and cutting vectors

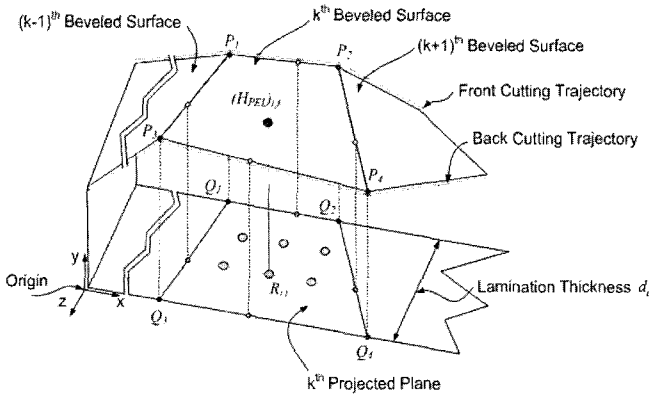

Fig. 12 Geometrical relationship for measuring $(H_{PEL})_{i,j}$ of the ruled and beveled top edge of a lamina

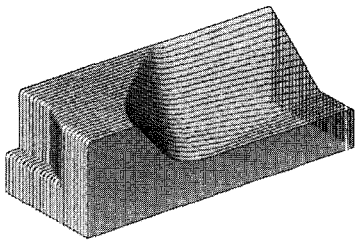

Fig. 13 Profiles of slicing planes for a part of the PEL tool

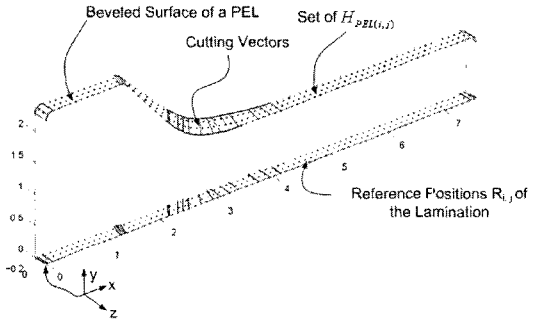

Fig. 14 Measured $(H_{PEL})_{i,j}$ on the beveled surface of a single profiled edge lamina

Table 2 Lamina thickness and dimensional error e_b results for the slicing example

Lamina Number	Profile Numbers Used	Thickness (mm)	Theoretical Dimensional Error (mm)
1	0, 2	6.4	0.10
2	2, 4	6.4	0.11
3	4, 6	6.4	0.12
4	6, 8	6.4	0.13
5	8, 10	6.4	0.16
6	10, 11	3.2	0.43
7	11, 13	6.4	0.05
8	13, 14	3.2	0.06
9	14, 15	3.2	0.84
10	15, 17	6.4	0.05
11	17, 19	6.4	0.04
12	19, 21	6.4	0.05
13	21, 23	6.4	0.05
14	23, 24	3.2	0.10

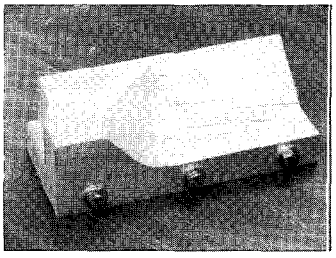

Fig. 15 A 14-lamina test section of a PEL tool

Stock lamina thicknesses of 3.18 and 6.35 mm (0.125" and 0.25") and an allowable error e_a = 0.25 mm (0.01") were chosen. Therefore, the standard increment thickness was 3.18 mm and profile polylines were generated every 3.18 mm perpendicular to the slicing reference plane, as shown in Fig. 13. The measured surface positions of the original CAD model $(H_{CAD})_{ij}$ with a matrix spacing δ of 1.92 mm (0.075") and the top surface of CAD model are presented in Fig. 10(b). Figure 14 shows the $(H_{PEL})_{ij}$ points at corresponding grid locations for one particular lamina. The software used both sets of measurements to determine the most appropriate lamina thicknesses. The slicing results for the *Test Section* using the adaptive slicing

algorithm outlined in Table 1 are given in Table 2. Since the CAD model was sliced 24 times using a constant 3.18-mm increment before implementing the actual slicing algorithm (as previously discussed), the profiles used to define each lamina are shown in the second column of this table. Except for Laminae #6 and #9, the calculated dimensional errors e_b using Eq. 2 for all laminae chosen by the algorithm were below the 0.25-mm error limit. The 0.43-mm and 0.84-mm errors for Laminae #6 and #9, respectively, occurred because the thinnest stock lamina available t_{min} was 3.18 mm. Conversely, Lamina #1 had a dimensional error of only 0.01 mm and could still be made thicker, but t_{max} was set to 6.35 mm (0.25"). All three situations demonstrated the limitations of having to specify stock lamina thicknesses. Based on the results of the adaptive slicing algorithm, cutting trajectories were created. Each of the 14 laminae was AWJ-cut and bolted together, as shown in Fig. 15.

5. Conclusions

We developed a new adaptive CAD slicing algorithm specifically for PELs to help advance the PEL tool development process. After a CAD model of the initial tool surface was chosen based on the part shape and manufacturing process to be used, it was directly sliced layer-by-layer based on available stock lamina thicknesses. Two errors were used by the algorithm to determine the appropriate slice thickness: the dimensional error (e_t), used to restrict the chordal deviation between the CAD model profiles and the actual polyline cutting trajectories used for the PEL tool, and the volumetric shape error index (e_b), used to compare the top beveled edge of each PEL with the true surface of the CAD model. Although the dimensional error (e_b) may be affected by the number of reference positions used and the local surface geometry of the tool surface, we believe it to be an effective index for evaluating beveled surfaces such as that of a PEL tool because a high-resolution matrix of points can be used. The adaptive slicing algorithm found optimal lamina thicknesses for the PEL tool.

A case study demonstrated how the algorithm works for the design and fabrication of a PEL tool. A difficult section of an actual industrial hydroforming tool was made using a PEL construction. To simplify the fabrication process, the available lamination stock sizes were limited to two thicknesses. The algorithm was successfully demonstrated for this case study, and the restrictions imposed by a limited set of lamina thicknesses were revealed. The volumetric shape error could exceed the specified limit because of the minimum thickness chosen. Finally, the tool section was fabricated by AWJ-cutting of individual lamina, which were then bolted together.

REFERENCES

1. Hull, C. W., "Apparatus for Production of Three-Dimensional Objects by Stereolithography," U.S. Patent No. 4575330, 1986.
2. Pham, D. T. and Dimov, S. S., "Rapid Manufacturing: The Technologies and Applications of Rapid Prototyping and Rapid Tooling," London: Springer–Verlag, 2001.
3. Walczyk, D. F. and Hardt, D. E., "A New Rapid Tooling Method for Sheet Metal Forming Dies," Proceedings of the 5th International Conference on Rapid Prototyping (Dayton, OH), pp. 275-289, 1994.
4. Walczyk, D. F. and Hardt, D. E., "Rapid Tooling for Sheet Metal Forming Using Profiled Edge Laminations: Design Principles and Demonstration," Journal of Manufacturing Science and Engineering, Vol. 120, pp. 746-754, 1998.
5. Murakawa, M., Miyazawa, H., Kobayashi, N. and Ohkawa, K., "Oblique Profile Cutting by Laser," Proceedings of LAMP '87 (Osaka, Japan), pp. 255-260, 1987.
6. Armillotta, A., Monno, M. and Moroni, G., "Rapid Waterjet," Jetting Technology, pp. 59-71, 1998.
7. Suh, Y. S. and Wozny, M., "Adaptive Slicing of Solid Freeform Fabrication Processes," Solid Freeform Fabrication Proceedings, pp. 404-411, 1994.
8. Kulkarni, P. and Dutta, D., "Adaptive Slicing of Parameterizable Algebraic Surfaces for Layered Manufacturing," Proceedings of the ASME Design Engineering Technical Conference, pp. 211-217, 1995.
9. Zhao, Z. and Laperriere, L., "Adaptive Direct Slicing of the Solid Model for Rapid Prototyping," International Journal of Production Research, Vol. 38, pp. 69-83, 2000.
10. Huang, X., Gu, P. and Zernicke, R., "Localization and Comparison of Two Free-Form Surfaces," Computer-Aided Design, Vol. 28, pp. 1017-1022, 1996.
11. Kase, K., Makinouchi, A., Nakagawa, T., Suzuki, H. and Kimura, F., "Shape Error Evaluation Method of Free-Form Surfaces," Computer-Aided Design, Vol. 31, pp. 495-505, 1999.
12. Hur, S. M. and Lee, S. H., "Study on the Reconstruction of Skull Prototyping Using CT Image and Laser Scanner," International Journal of the Korea Society for Precision Engineering, Vol. 1, No. 1, pp. 146-151, 2000.
13. Yoo, S., "Development of an Advanced Design Process for Profiled Edge Laminated Tooling," Ph.D. dissertation, Dept. of Mechanical, Aerospace, and Nuclear Engineering, Rensselaer Polytechnic Institute, 2003.
14. Im, Y. T. and Walczyk, D. F., "Development of a Computer-Aided Manufacturing System for Profiled Edge Lamination Tooling," Journal of Manufacturing Science and Engineering, Vol. 124, pp. 754-761, 2002.
15. Brown, K., "Implementation of the Profiles Edge Laminations Tooling Process through Manufacturing Case Study," MS thesis, Dept. of Mechanical, Aerospace and Nuclear Engineering, Rensselaer Polytechnic Institute, 2002.